The Journal of Experimental Biology 213, 2303-2309

doi:10.1242/jeb.039206

Motor patterns associated with crawling in a soft-bodied arthropod

Michael A. Simon, Steven J. Fusillo, Kara Colman and Barry A. Trimmer*

Department of Biology, 163 Packard Avenue, Tufts University, Medford, MA 02155, USA

*Author for correspondence (barry.trimmer@tufts.edu)

Accepted 26 March 2010

SUMMARY

Soft-bodied animals lack distinct joints and levers, and so their locomotion is expected to be controlled differently from that of animals with stiff skeletons. Some invertebrates, such as the annelids, use functionally antagonistic muscles (circumferential and longitudinal) acting on constant-volume hydrostatics to produce extension and contraction. These processes form the basis for most theoretical considerations of hydrostatic locomotion in organisms including larval insects. However, caterpillars do not move in this way, and their powerful appendages provide grip independent of their dimensional changes. Here, we show that the anterograde wave of movement seen in the crawling tobacco hornworm, *Manduca sexta*, is mediated by co-activation of dorsal and ventral muscles within a body segment, rather than by antiphasic activation, as previously believed. Furthermore, two or three abdominal segments are in swing phase simultaneously, and the activities of motor neurons controlling major longitudinal muscles overlap in more than four segments. Recordings of muscle activity during natural crawling show that some are activated during both their shortening and elongation. These results do not support the typical peristaltic model of crawling, but they do support a tension-based model of crawling, in which the substrate is utilized as an anchor to generate propulsion.

Key words: *Manduca sexta*, motor pattern, kinematics, insect, locomotion.

INTRODUCTION

In contrast with animals having hard skeletons, soft-bodied creatures are deformable, can perform precise movements in almost limitless orientations and can thereby access resources that are otherwise difficult to reach. Understanding the control of this flexibility and versatility is a challenging problem because the central nervous system (CNS) must coordinate movements with many degrees of freedom, but without easily defined joints where sensors could provide force and feedback on position.

Manduca sexta is an advantageous subject for the study of soft-bodied coordination because its neural and biomechanical components are easily accessible. Each abdominal segment contains about 70 distinct muscles (Barth, 1937; Beckel, 1958; Eaton, 1988), each innervated by just one (occasionally two) motoneuron(s), and there are no inhibitory motor units (Taylor and Truman, 1974; Levine and Truman, 1985). Therefore, most of the movements of *Manduca* are controlled by only a few hundred motoneurons, whose activity can be monitored using electrodes implanted in the muscles of freely moving animals. The muscle attachment points have been mapped to external features, permitting kinematic muscle length measurements, and also providing an accurate site for electrode placement (Fig. 1A).

Caterpillars lack circular muscle, do not maintain constant segment volume (Trimmer and Issberner, 2007) and do not constrict body segments in the way that worms do (Snodgrass, 1961; Trimmer and Issberner, 2007). Instead, *Manduca* crawls by means of a wavelike series of segmental contractions starting at the posterior and moving forwards. Most of the crawl cycle and propulsion is generated by the abdominal segments, with up to three segments in swing phase simultaneously, and the prolegs carried forwards passively (Belanger and Trimmer, 2000; Trimmer and Issberner, 2007). During stance, the prolegs grip the substrate passively (Mezoff et al., 2004) using cuticular hooks (crochets), which are actively retracted just after the start of the segment swing phase (Belanger et al., 2000). Unlike in burrowing or swimming annelids and marine cephalopods, *Manduca* movements are entirely terrestrial, comparatively slow and usually confined to a small workspace, facilitating video and optical tracking analysis.

The most prevalent explanation of how caterpillars crawl is based entirely on anatomical data and visual descriptions of the movements (Barth, 1937). It was proposed that different muscle layers (internal and external) serve different roles in maintaining turgor or driving movements. In this model, crawling comprises three distinct stages: (1) contraction of dorsal longitudinal muscles to raise the posterior segment, (2) contraction of ventral turgopleural muscles to raise the ventral body wall and prolegs, and (3) contraction of ventral longitudinal muscles to lower the posterior segment so that the prolegs can make contact with the substrate. This description supposes that dorsal and ventral muscles in a body segment are activated out of phase with one another and that activation of similar muscles in adjacent segments progresses sequentially. This mechanism is repeated in many entomology and biomechanics textbooks (e.g. Wigglesworth, 1950; Hughes, 1965; Douglas, 1986; Chapman, 1998). However, there is little direct evidence for this mechanism, which does not necessarily explain how body segments are carried forwards.

The current study takes advantage of the nearly one-to-one motoneuron-to-muscle mapping of *Manduca sexta* to examine systematically the control patterns associated with movements. By measuring activity from multiple muscles simultaneously, we found that the control of caterpillar crawling is not organized into discrete, segment-by-segment waves of longitudinal muscle activity; instead, it consists mainly of anteriograde, phase-delayed co-activation of abdominal muscles. Furthermore, dorsal and ventral muscles in each segment are also co-active – so antagonistic motor timing is not responsible for the wave of lifting and axial bending. These findings are consistent with a new view of caterpillar biomechanics in which

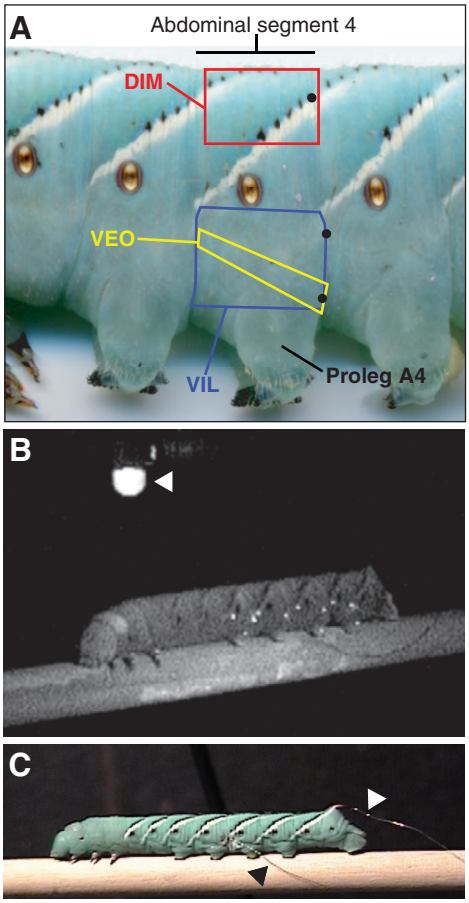

Fig. 1. (A) Map of body wall muscles to external features. The positions of the dorsal interior medial (DIM), ventral exterior oblique (VEO) and ventral internal longitudinal (VIL) muscles are illustrated for the fourth abdominal segment. The EMG wire insertion points are indicated by black circles. Anterior is to the left; dorsal is at the top. (B) View of crawling caterpillar under UV illumination. Ultraviolet illumination causes markers on the cuticle to fluoresce, seen here as small glowing dots. The white arrowhead denotes the LED used to synchronize the videos and EMG data. One electrode is also visible as a black line against the dowel. (C) Thin (25 μm diameter), twisted-pair nichrome wires were inserted into the cuticle and drawn back or up and away from the animal so as not to impede movement. The black arrowhead points to an electrode implanted into A4 VIL. The white arrowhead points to the silver ground electrode implanted into the dorsal horn of the animal.

abdominal muscles generate tension within the body of the animal through the proleg and create compressive forces on the substrate. According to this scheme, crawling consists of axial generation of muscle forces and coordination of proleg grip release, producing highly stable forwards propulsion.

MATERIALS AND METHODS

Raising *Manduca*

Larvae of the tobacco hornworm *Manduca sexta* (Lepidoptera: Sphingidae, L.) were individually raised to the fifth instar (Bell and Joachim, 1976). Animals were kept at a constant temperature of 26°C in a light:dark cycle of 17 h:7 h and fed with an artificial diet. Fifth-instar animals were used on the first or second day of the instar.

Three-dimensional motion-capture

The strain cycling of muscles was monitored relative to the body movements during upright horizontal crawling. Precisely defined points on the body surface corresponding to muscle attachments (Fig. 1) (Levine and Truman, 1985) were labeled with fluorescent latex spheres (160 μm diameter, Duke Scientific, Palo Alto, CA., USA, Cat. No. 35–14) and glued in place using silicone rubber clear aquarium sealant (Dow Corning, Midland, MI, USA). Markers were also placed on the lateral distal surface of the prolegs, whose horizontal velocity was used to define the swing and stance phases of each segment (see 'Crawl timing' section, below).

The freely moving larvae were illuminated with a high-intensity longwave ultraviolet lamp (Blak-Ray, Upland CA, USA, Model B-100A) and their movements recorded using two Canon ZR10 digital video cameras positioned anteriorly and posteriorly approximately 45 deg to the axis of movement (Fig. 1B). A small light-emitting diode (LED) and a fluorescent fixed point were always in the field of view for both cameras. A brief (18 ms) LED flash was used to synchronize the recorded data on each camera. All movements are described relative to an external three-dimensional calibration frame placed in the view of both cameras with the x-axis aligned along the direction of crawling. The y-axis describes movements in the dorso-ventral plane and the z-axis describes movements in the lateral plane.

Data were analyzed only for sequences of steps in which the markers were clearly visible in both cameras, although frame averaging was used to enhance marker visibility in some cases. Using microspheres or fixed-body features as reference points, recorded video sequences were digitized in kinematic software – either Ariel performance analysis system (APAS; Ariel Dynamics, San Diego, CA, USA) at seven frames per second, or DLTdv3 (Hedrick, 2008) at 30 frames per second – and converted to three-dimensional positions using the direct linear transform. Axial velocities (V_x) were calculated from changes in axial position (e.g. Fig. 2A). All data reported here are from spontaneous bouts of crawling rather than from provoked movements.

Electromyography

Bipolar electromyography (EMG) electrodes were fabricated by soldering a pair of intertwined insulated nichrome wires of diameter 25 μm to adjacent terminals of a male nine-pin connector. The tip of the wire was cleaned, cut at a 45 deg angle for increased surface area and dipped in an orange fluorescent powder. A fine pin was used to make a small hole at the posterior attachment point of the target muscle, and the electrode was inserted 0.1–0.2 mm into this hole and sealed using a veterinary adhesive (Vetbond, 3M, St Paul, MN, USA) (Fig. 1C). A small portion of the dorsal horn (1–2 mm) was cut off, and a fine silver grounding wire was inserted into the horn and sealed with Vetbond. The electrode wires were connected to differential inputs of an amplifier (AM-System, model 1700), and signals were amplified 10,000-fold with cutoff filters at 10 Hz and 10 KHz. Data were digitized at 3333 samples per sec per channel (Model DI720, Dataq Instruments).

Muscle activity was expressed for most experiments as an activity index (AI; for example, Fig. 3A), obtained by subtracting the raw EMG voltage recordings from the mean, and then rectifying and averaging the resulting voltages into 100 ms bins (DataView, W. J. Heitler, Univ. St Andrews, UK). Because of small differences in the position and resistance of the electrodes, the absolute magnitude of the voltage signal varied between preparations. For this reason, all comparisons between different animals or trials

aggregate and compare the timing, rather than the amplitude, of EMG activity.

Data analysis

Definitions of crawling

Manduca crawling consists of a repeated sequence of stepping motions spanning the entire body length. For the purpose of this analysis, a crawl is defined as a contiguous series of proleg movements and segment contractions proceeding from the rear of the animal to the front. Crawls are initiated when the terminal prolegs release the substrate and end at the start of the next crawl. Within a crawl, each body segment takes a single step in anteriograde progression. Steps are therefore always reported for particular segments. Each step consists of a stance phase and a swing phase, which in proleg-bearing segments correspond to gain and loss of contact with the substrate, respectively (the measurement of these phases is described below). A bout of crawling consists of multiple crawls occurring in succession.

Crawl timing

Although a crawl can be initiated immediately following the end of the previous crawl, this is not always the case. The pause between successive crawls can be highly variable. This has the effect of imparting variation to the step duration of a single body segment during a bout of crawling. The timing of steps between different segments within a crawl is far less variable (see Fig. 2C). This relationship was confirmed by regressing swing phase duration (defined below) against log-transformed crawl period, determined by the interval between proleg swing velocity peaks. (One animal was omitted from analysis owing to demonstrating excessive pauses well beyond normal.) Based on this relationship between step timing and crawl speed, the timings of kinematic and EMG events averaged over multiple crawls and different individuals are reported relative to the peak and duration of the third abdominal (A3) proleg swing phase, as defined below.

Calculating swing phase

The swing phase of each step was defined by a non-zero axial proleg velocity (V_x); conversely, stance phase was defined as the period between these sharp velocity peaks, during which there is little to no axial proleg movement. The point of maximum V_x during the swing phase, or swing peak, was used as an unambiguous reference time for aligning events to be averaged. Each swing peak was identified after Loess smoothing (1 degree, parameter 0.1) of the kinematic data. All subsequent aggregations and alignments were carried out using the raw (unsmoothed) data. Kinematic data for each step in a bout of crawling were aligned using the swing peak as t=0 s. The average swing profile for multiple steps was then calculated as the mean V_x in a window centered on t=0 s, typically 2 or 3 s before and after the swing peak. The duration of the swing phase was measured by fitting the mean proleg swing profile with a five-parameter Weibull curve (R^2>0.98) and calculating the width of this curve at 10% of the peak amplitude.

EMG alignment

The A3 proleg swing period was a consistent measure of overall crawl period (Fig. 2C) and was used to normalize data over multiple crawls and from multiple individuals. Comparisons of activity index (AI) timing across muscles, segments and individuals were calculated in a similar manner to that described for the swing phase measurements (Figs 3 and 5). EMG data were first aligned to peak swing times in segment A3. These aligned data were averaged to generate the mean AIs for each of the observed muscles in each bout of crawling. Each mean AI was fitted with a five-parameter Weibull curve. The timing of peak EMG activity and onset and offset of EMG activity were identified as times at which the fitted Weibull curve reached peak and 10% peak amplitudes. These raw times were divided by half the A3 proleg swing duration to yield a swing normalized time (T_s) that is zero at the peak of swing, –1 at the start of swing and +1 at the end of swing. Muscles and segments were compared for changes in activity onset, peak or offset using Student's t-test of paired samples or analysis of variance (ANOVA). As three comparisons were completed for each sample – activity onset, peak and offset – Bonferroni's *post-hoc* adjustment for multiple comparisons was used, and significance was assumed at $P<\alpha_c=\alpha/n=0.05/3=0.017$.

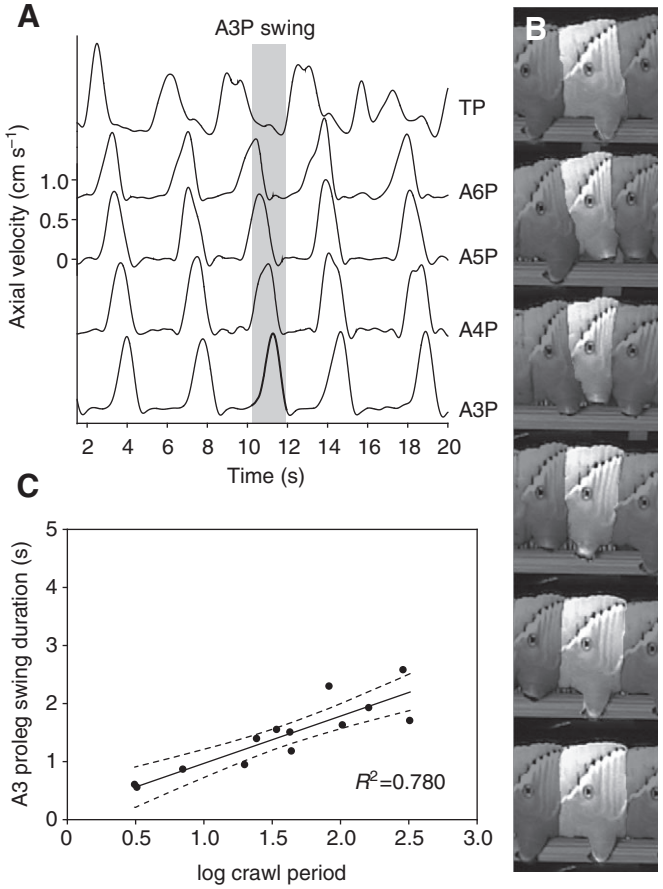

Fig. 2. The relationship of segmental swing and stance phases to the overall crawling period. (A) In a series of five successive crawls, each segment takes a single step consisting of swing (positive peak) and stance phases, here represented by proleg axial velocity. The wave of movement progresses forwards from the terminal prolegs (TPs) through the abdominal prolegs in segments six to three (A6P–A3P) and into the thoracic and head segments (not shown). The timing of one A3P swing phase is shaded across segments for comparison. The variability in TP velocity was a consistent finding (see also Trimmer and Issberner, 2007). Data are from a single, representative animal. (B) Pictorial sequence of A4 segment (highlighted) from stance phase through swing phase to stance phase (Simon and Trimmer, 2009). (C) The A3P swing duration calculated from multiple crawls in 13 animals (see 'Calculating swing phase' section in Materials and methods). Swing duration is shown regressed against log-transformed crawl period (s) (linear regression, N=13, R^2=0.780, P<0.0005). Dashed lines represent 95% confidence intervals.

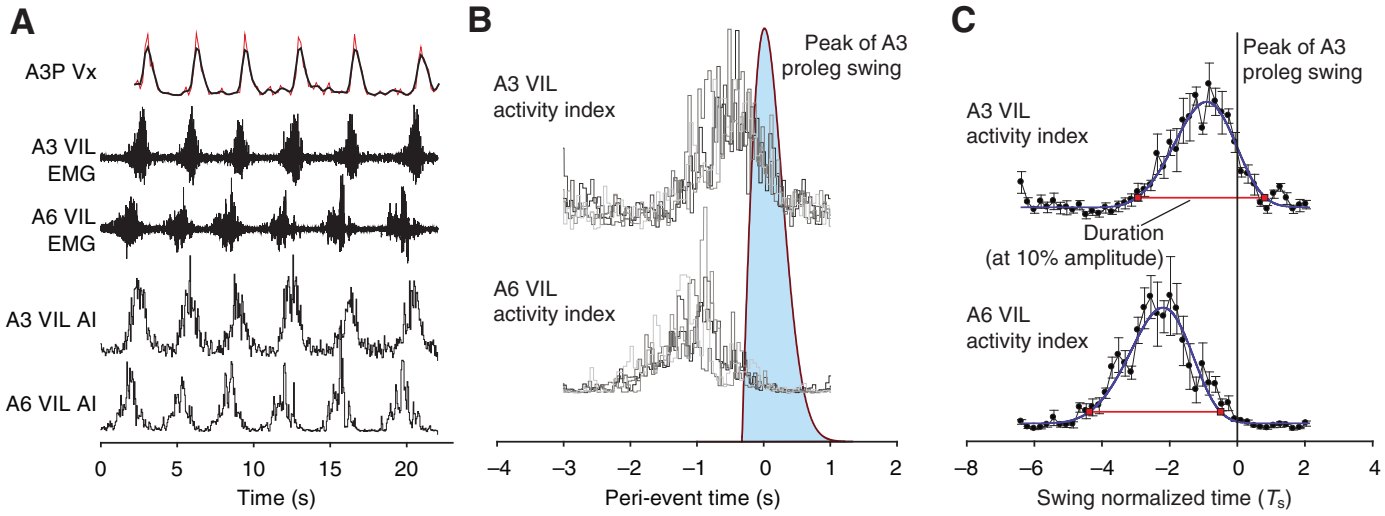

Fig. 3. Intersegmental EMG timing and duration. (A) The raw and filtered axial velocity (V_x) of A3P recorded for six successive steps in one representative animal (top trace, red and black traces, respectively) with concurrent EMGs from muscle VIL in segments A3 and A6 (middle traces). The activity indexes (AIs) for the EMGs are shown in the lower traces. (B) The AIs were aligned relative to the peak V_x and are shown with the swing phase defined by the mean V_x of A3P (blue-shaded curve). (C) The mean duration and timing of the AIs for the complete series of steps were calculated relative to the A3 proleg swing duration (swing normalized time, see text). Error bars represent ± s.e.m.

RESULTS

Crawl period and swing duration

Crawling consisted of waves of movement beginning in the terminal segment and progressing anteriorly through the abdomen into the thorax. The first part of this movement was monitored by tracking the axial velocity (V_x, i.e. along the direction of travel) of the prolegs in each body segment (Fig. 2). During bouts of fast crawling, the initiation of swing in the terminal prolegs (TPs) occurred before or immediately after the onset of stance in the third abdominal proleg (A3P, Fig. 2A); hence a new wave was initiated as the previous one passed through the thorax. In other cases, there was a longer delay between each crawl (data not shown). Despite the variable delay between initiated waves, once a wave was initiated, it proceeded with a consistent velocity that correlated with the average crawl period for a bout of crawling (Spearman's rank correlation, N=13, ρ=0.901, P<0.0005) (Fig. 2C). Therefore, when data were compiled for multiple animals, they were normalized to the A3 proleg swing period rather than to the duration of the crawl. This avoided data distortion that would occur when crawl initiation was delayed during a bout of crawling.

Inter-segmental muscle activity

Simultaneous EMG recordings were made from VIL in segments A3 and A6 during spontaneous crawling. The EMG activity in each muscle was converted to an activity index (Fig. 3A) and recordings for successive steps aligned to the peak of the proleg swing phase in A3 (Fig. 3B). The mean AI for each muscle in a bout of crawling was then calculated and normalized to the A3 swing phase duration (Fig. 3C). Across six animals, the onset of activity in A3 VIL occurred before the beginning of A3 swing phase, and the offset of activity in A3 VIL occurred at the end of, or slightly before the end of, the A3 swing phase (Fig. 4). In each body segment, VIL EMG activity ceased approximately at the end of the swing phase. The onset, peak and offset of activity in A6 VIL preceded those of A3 (paired Student's t-tests, d.f.=5, for onset: P=0.0177; for peak: 0.0055; for offset: 0.0096). However, there was considerable overlap of activity in VIL in A3 and A6, such that the peak of EMG activity in A6 coincided with the onset of activity in A3 (Fig. 4). This is consistent with the overlap in timing of the swing phase in these two segments (Fig. 2A).

Intra-segmental muscle activity

Simultaneous recordings were made of EMG activity in the dorsal internal medial (DIM) muscle and either the ventral internal longitudinal (VIL) or the ventral external oblique (VEO) muscle on the same side of segment A4. The EMG activity in each muscle was converted to an activity index (Fig. 5A), and the mean AI for each muscle in a bout of crawling was again aligned to the A3 proleg swing peak (Fig. 5B) and normalized to the A3 swing phase duration (Fig. 5C). Throughout all steps and across all animals, dorsal and ventral muscles were coactive (Fig. 6). There were no significant differences in timing of onset, peak or offset between the three muscles studied (one-way ANOVA, N=14, for onset: $F_{0.05(2,11)}$=1.167, P=0.347; for peak: $F_{0.05(2,11)}$=2.243, P=0.152; for offset: $F_{0.05(2,11)}$=1.537, P=0.258). Despite a trend towards earlier onset of activity in the dorsal muscle DIM compared with that in the ventral muscles VEO and VIL, there was no significant difference in the timing of activity between dorsal and ventral muscles (linear contrast of dorsal versus ventral muscle timing,

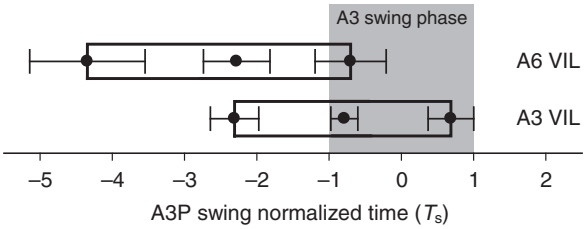

Fig. 4. The relative timing and duration of VIL EMG activity in segments A6 and A3 during spontaneous crawling. The times of EMG onset, peak activity and offset are plotted relative to the time and duration of the swing phase of the A3 proleg (gray bar). Values are means (±s.e.m.) for six animals (5–10 steps each).

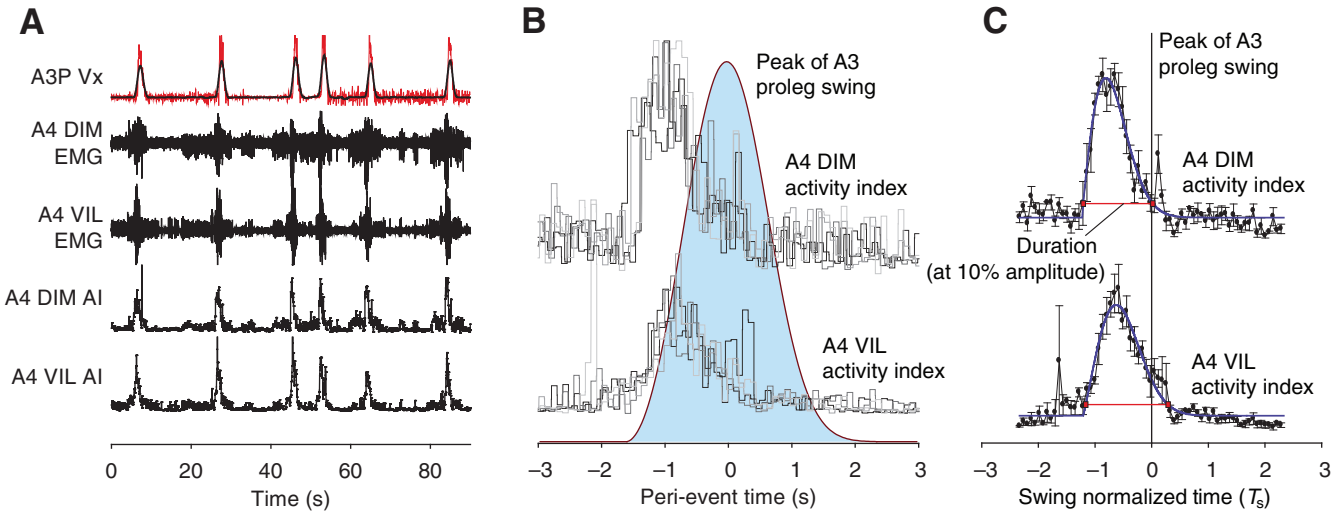

Fig. 5. Intrasegmental EMG timing and duration. (A) The raw and filtered axial velocity (V_x) of A3P recorded for six successive steps in one representative animal (top trace, red and black traces, respectively) with concurrent EMGs from muscles DIM and VIL in segment A4 (middle traces). The activity indexes (AIs) for the EMGs are shown in the lower traces. (B) The AIs were aligned relative to the peak of the swing phase at peri-event time equal to zero. (C) The mean duration and timing of the AIs for this complete series of steps were calculated relative to the A3 proleg swing duration (swing normalized time, see text). Error bars represent ± s.e.m. Concurrent EMG recordings of A4 DIM and A4 VEO were processed in the same manner (data not shown).

d.f.=11, N=14, for onset: t=1.527, P=0.155; for peak: t=1.206, P=0.253; for offset: t=–0.143, P=0.889).

DISCUSSION

Although soft-bodied animals are common, relatively little is known about the control of their movements. This is partially because movements in highly compliant animals are characterized by many degrees of freedom, often referred to as 'hyper-redundant' systems (Shammas et al., 2003), and by the large number of factors (e.g. muscle length, muscle tension, body volume and hydrostatic pressure) that might need to be coordinated for predictable and repeatable movements. Furthermore, soft-bodied crawling is relatively inefficient and slow. The energy requirement of soft-bodied locomotion over a fixed distance is approximately 4–10 times that of arthropods and vertebrates using rigid skeletons (Casey, 1991; Berrigan and Lighton, 1993), and telescopic locomotion speeds are 10–20% of those of adult insects running and walking (Berrigan and Pepin, 1995). Despite this cost in speed and efficiency, crawling by larval arthropods is evolutionarily successful because it allows them to exploit specialized environmental niches. Here, we begin to address the question of how such a system is controlled in the base case of spontaneous forwards crawling.

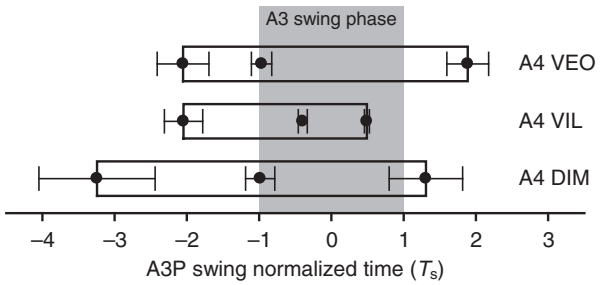

Fig. 6. The relative timing and duration of EMG activity in three muscles in segment A4 during spontaneous crawling. The times of EMG onset, peak activity and offset are plotted relative to the time and duration of the A3 proleg swing phase (gray bar). Values are means (±s.e.m.) for 3–7 animals (5–10 steps each).

The current 'peristaltic' model of caterpillar crawling

Although the prevailing descriptions of caterpillar crawling are based on peristalsis (Holst, 1934; Barth, 1937), both kinematic data (Trimmer and Issberner, 2007) and the current findings on motor neuron activity reveal a different mechanism. Our results show that muscles in posterior segments are activated before those in anterior segments, as predicted by observation (Barth, 1937) and demonstrated by fictive crawling in isolated nerve chords (Johnston and Levine, 1996). However, activity in the major ventral longitudinal muscles of different segments overlaps substantially, such that muscles in posterior segment A6 are still active at the peak of activity in A3 just as the A3 proleg swing phase begins (Fig. 4). This means that the large intra-segmental muscles are active in at least four abdominal segments simultaneously.

With regard to the coordination of muscles within a segment, Barth's model predicted that dorsal muscle activity would precede (or alternate with) ventral muscle activity. Our results show that, although activity in the dorsal internal medial (DIM) tends to begin before that of the ventral muscles (VIL and VEO), the delay is not significant and the major ventral and dorsal muscles are mostly coactive. Additionally, Barth's model suggested that ventral muscles are active only at the end of the swing phase to bend the front of the crawling wave ventrally. However, we found that A3 VIL becomes active before the A3 swing phase begins and peaks at the onset of the A3 proleg swing phase. Even accounting for the stimulus–contraction delay in this muscle (Woods et al., 2008), active tension in VIL is presumably declining throughout its own forwards movement.

A new model for neural control of tension-based crawling

Given that the anatomy, kinematics and motor patterns of crawling are not consistent with a hydrostatic peristalsis mechanism, what is the source of propulsion for a crawling caterpillar? The most likely explanation is one provided by the eminent entomologist Robert

Evans Snodgrass (1875–1962) in his monograph *The Caterpillar and the Butterfly* (Snodgrass, 1961). Snodgrass dismissed the idea that caterpillar crawling is peristaltic, noting that "other writers…have attributed the caterpillars' movements to contraction of the segments without noting the expansion." Instead, he declared that forwards motion is achieved by "each contracting segment expanding the segment behind in a forward direction". Although Snodgrass provided no evidence or citation for his interpretation, our studies support this mechanism and provide for a more detailed explanation (Fig. 7). Measurements of normal and axial ground reaction forces (GRFs) in multiple prolegs during horizontal crawling show that *Manduca* exerts compressive forces on the substrate between anterior and posterior contact points (Lin and Trimmer, 2010). In doing so, *Manduca* can develop tension within its body that is then released to move segments forwards during the swing phase of a step. This use of (relatively) stiff substrates to locomote, called an 'environmental skeleton', has the advantage that it does not require body stiffening by high internal pressure. Data on axial GRFs indicate that, during the A4 swing phase, tension is generated between posterior prolegs (on the terminal or A6 segments) and anterior contact points such as the prolegs in A3 or the thoracic legs. Our results show the large longitudinal muscles in mid-abdominal segments are co-active during this stage, presumably generating longitudinal tension that pulls segments forwards as they enter the swing phase. Given that a single VIL muscle from a 2 g *Manduca* produces a peak force of 40 mN (about 4 g) (Woods et al., 2008), activation of multiple longitudinal muscles in a single segment is capable of developing sufficient tension to move the mass of the body upon proleg release.

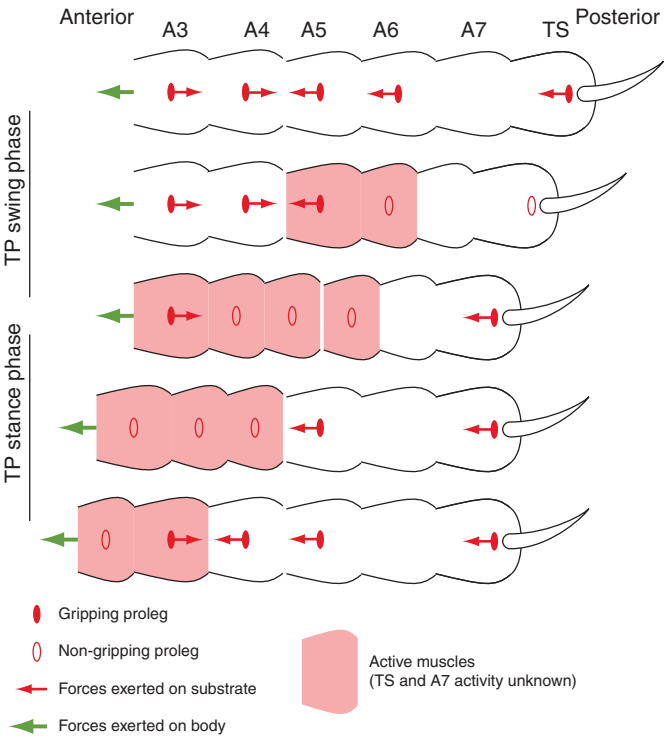

Fig. 7. Schematic of tension-based crawling model. The crawling caterpillar generates compressive forces on the substrate (red arrows) through the prolegs (filled ovals when gripping, empty ovals when released), resulting in tension within the body [abdominal segments 3–7 (A3–A7) and terminal segment (TS) shown]. During the terminal proleg (TP) swing phase, the TPs release from the substrate and are drawn forwards by tension generated within anterior body segments. During TP stance phase, coactive longitudinal muscles (shaded red) generate tension within proleg-bearing abdominal segments, which are drawn forwards when their prolegs release the substrate. Thoracic segments generate constant forwards force on the abdomen (green arrows). The muscle activity data for abdominal segments A3–A6 are from Figs 4 and 6. The force generation data are from Lin and Trimmer (Lin and Trimmer, 2010).

Based on those results, we can identify the source of most propulsion in caterpillar crawling as the contraction of muscles in more anterior segments, thus generating tension, and by rotation of the terminal segment around its attachment point before the A6 stance phase. Despite the visual impression of wave initiation by the terminal segment, our results and GRF measurements suggest that the terminal prolegs play a more important role in anchoring the body than in 'pushing' the next segment forwards. This interpretation is supported by the results of sectioning the ventral connective between the A6 and terminal ganglia. In such animals, the terminal segment is dragged passively during a crawl, but the anterograde wave is initiated at A6 and otherwise appears normal (Holst, 1934; Trimmer and Issberner, 2007). The crucial element of crawling is therefore the coordinated timing of tension changes in the abdomen and the sequenced release of crochets from the substrate.

Finally, a complete interpretation of the motor patterns that underlie *Manduca* crawling can only be achieved by considering the biomechanics of the moving tissues and fluids. This must include both active and passive properties of muscles (Dorfmann et al., 2007; Dorfmann et al., 2008; Woods et al., 2008), the anisotropic behavior of the body wall (Lin et al., 2009), mechanics and control of crochet gripping and release (Belanger et al., 2000) and the movements of internal tissues and fluids (M.A.S., W. A. Woods, Y. J. Serebrenik, S. M. Simon, L. I. van Griethuijsen, J. J. Socha, W. K. Lee and B.A.T., unpublished). One of our goals is to build a structural model of Manduca that includes constitutive material properties based on large deformation theory (e.g. Dorfmann et al., 2007; Dorfmann et al., 2008; Lin et al., 2009). By applying natural motor commands to this model, it will be possible to explore how interactions between the nervous system and morphology (Chiel and Beer, 1997; Pfeifer, 2000) help to control movements in soft-bodied animals.

LIST OF SYMBOLS AND ABBREVIATIONS

A1–A7	abdominal segments 1 through 7
A3P	proleg on third abdominal segment
APAS	Ariel performance analysis system
D	dark
DIM	dorsal internal medial muscle
L	light
T1–3	thoracic segments 1 through 3
TP	terminal proleg
TS	terminal segment
VEO	ventral external oblique muscle
VIL	ventral internal longitudinal muscle

ACKNOWLEDGEMENTS

This work was funded by NSF/IBN grant 0117135 to B.T. We thank Faith Hester for helpful discussions and additional assistance.

REFERENCES

Barth, R. (1937). Muskulatur und Bewegungsart der Raupen. *Zool. Jb. Physiol.* **62**, 507-566.
Beckel, W. E. (1958). The morphology, histology and physiology of the spiracular regulatory apparatus of *Hyalophora cecropia*. *Proceedings of the 10th International Congress of Entomology* **2**, 87-115.
Belanger, J. H. and Trimmer, B. A. (2000). Combined kinematic and electromyographic analyses of proleg function during crawling by the caterpillar *Manduca sexta*. *J. Comp. Physiol. A* **186**, 1031-1039.
Belanger, J. H., Bender, K. J. and Trimmer, B. A. (2000). Context-dependency of a limb-withdrawal reflex in the caterpillar *Manduca sexta*. *J. Comp. Physiol. A* **186**, 1041-1048.

Bell, R. A. and Joachim, F. G. (1976). Techniques for rearing laboratory colonies of tobacco hornworms and pink bollworms Lepidoptera-sphingidae-gelechiidae. *Ann. Entomol. Soc. Am.* **69**, 365-373.
Berrigan, D. and Lighton, J. R. (1993). Bioenergetic and kinematic consequences of limblessness in larval Diptera. *J. Exp. Biol.* **179**, 245-259.
Berrigan, D. and Pepin, D. J. (1995). How maggots move: allometry and kinematics of crawling in larval diptera. *J. Insect Physiol.* **41**, 329-337.
Casey, T. M. (1991). Energetics of caterpillar locomotion: biomechanical constraints of a hydraulic skeleton. *Science* **252**, 112-114.
Chapman, R. F. (1998). *The Insects: Structure and Function.* Cambridge, UK: Cambridge University Press.
Chiel, H. J. and Beer, R. D. (1997). The brain has a body: adaptive behavior emerges from interactions of nervous system, body and environment. *Trends Neurosci.* **20**, 553-557.
Dorfmann, A., Trimmer, B. A. and Woods, W. A., Jr (2007). A constitutive model for muscle properties in a soft bodied arthropod. *J. R. Soc. Interface* **4**, 257-269.
Dorfmann, A., Woods, W. A., Jr and Trimmer, B. A. (2008). Muscle performance in a soft-bodied terrestrial crawler: constitutive modelling of strain-rate dependency. *J. R. Soc. Interface* **5**, 349-362.
Douglas, M. M. (1986). *The Lives of Butterflies.* Ann Arbor, MI: University of Michigan Press.
Eaton, J. L. (1988). *Lepidopteran Anatomy.* New York: John Wiley and Sons.
Hedrick, T. L. (2008). Software techniques for two- and three-dimensional kinematic measurements of biological and biomimetic systems. *Bioinspir. Biomimet.* **3**, 34001.
Holst, E. V. (1934). Motorische und tonischeErregung und ihr Bahnenverlauf bei Lepidopteranlarven. *Zeitshrift fur vergleichende physiologie* **21**, 395-414.
Hughes, G. M. (1965). Locomotion: Terrestrial. In *The Physiology of Insecta*, vol. 2 (ed. M. Rockstein), pp. 227-253. New York City, NY: Academic Press, Inc.
Johnston, R. M. and Levine, R. B. (1996). Crawling motor patterns induced by pilocarpine in isolated larval nerve cords of *Manduca sexta*. *J. Neurophysiol.* **76**, 3178-3195.
Levine, R. B. and Truman, J. W. (1985). Dendritic reorganization of abdominal motoneurons during metamorphosis of the moth, *Manduca sexta*. *J. Neurosci.* **5**, 2424-2431.
Lin, H. T. and Trimmer, B. A. (2010). The substrate as a skeleton: ground reaction forces from a soft-bodied legged animal. *J. Exp. Biol.* **213**, 1133-1142.
Lin, H. T., Dorfmann, A. L. and Trimmer, B. A. (2009). Soft-cuticle biomechanics: a constitutive model of anisotropy for caterpillar integument. *J. Theor. Biol.* **256**, 447-457.
Mezoff, S., Papastathis, N., Takesian, A. and Trimmer, B. A. (2004). The biomechanical and neural control of hydrostatic limb movements in *Manduca sexta*. *J. Exp. Biol.* **207**, 3043-3053.
Pfeifer, R. (2000). On the role of morphology and materials in adaptive behavior. In *From Animals to Animats*, vol. 6 (ed. J.-A. Meyer, A. Berthoz, D. Floreano, H. Roitblat and S. W. Wilson), pp. 23-32. Cambridge: MIT Press,.
Shammas, E., Wolf, A., Brown, H. and Choset, H. (2003). New Joint Design for Three-dimensional Hyper Redundant Robots. In *IEEE/RSJ International Conference on Intelligent Robots and Systems*, vol. 4, pp. 3594-3599. Las Vegas, Nevada.
Simon, M. A. and Trimmer, B. A. (2009). Movement encoding by a stretch receptor in the soft-bodied caterpillar, *Manduca sexta*. *J. Exp. Biol.* **212**, 1021-1031.
Snodgrass, R. E. (1961). The caterpillar and the butterfly. *Smithsonian Miscellaneous Collections* **143**, 51.
Taylor, H. M. and Truman, J. W. (1974). Metamorphosis of the abdominal ganglia of the tobacco hornworm, *Manduca sexta*. *J. Comp. Physiol.* **90**, 367-388.
Trimmer, B. A. and Issberner, J. I. (2007). Kinematics of soft-bodied, legged locomotion in *Manduca sexta* larvae. *Biol. Bull.* **212**, 130-142.
Wigglesworth, V. B. (1950). *The Principles of Insect Physiology.* London, UK: Methuen.
Woods, W. A., Jr, Fusillo, S. and Trimmer, B. A. (2008). Dynamic properties of a locomotory muscle of the tobacco hornworm *Manduca sexta* during strain cycling and simulated crawling. *J. Exp. Biol.* **211**, 873-882.